Power Quality Enhancement of UPQC Connected WECS using FFA with RNN

Senthil Vadivu U
Department of Electrical and Electronics Engineering
PES Institute of Technology
Bangalore, India
senthilv@pes.edu

B K Keshavan
Department of Electrical and Electronics Engineering
PES Institute of Technology
Bangalore, India
keshavanbk@pes.edu

Abstract—**In this paper a design of combined operation of Unified Power Quality Conditioner (UPQC) and Wind Energy Conversion System (WECS) is presented to alleviate the power quality problems in distribution system. The integration of wind power into an electric grid encounters the Power Quality (PQ) problems and which will be minimized. The control strategy of UPQC is analyzed with adaptive technique, which is used for Firefly Algorithm (FFA) and Recurrent Neural Network (RNN). To optimize the control pulses to UPQC, FFA is used and the RNN is used to train the optimization parameter. The optimal control pulses are generated by the series and shunt Active Power Filters (APF) based on the source side and load side parameters. This approach is competent to inject the active power to grid in addition to its ability to improve the PQ in distribution system. The performance of the proposed FFA based UPQC system is validated through simulations using MATLAB/SIMULINK and compared with the existing techniques such as ANFIS support UPQC and GA support UPQC.**

Keywords—***Unified Power Quality Conditioner (UPQC), Wind Energy Conversion System (WECS), Power Quality (PQ), FFA (FireFly Algorithm), RNN (Recurrent Neural Network).***

I. INTRODUCTION

As a consequence of the synchronization of wind energy through the current power framework necessitates voltage control, soundness and power eminence problem. The concern of PQ is tremendous impact on the wind turbine [1, 2] and to minimize these issues a unification of series and shunt compensators recognized as the UPQC has been used.

The UPQC consists of shunt and series active power filters and a dc interface capacitor. The utility of the dc interface capacitor is to maintain constant voltage among the two active filters. Due to longer discharge time, the voltage administration time of capacitor is too elevated. According to the consequence of long discharge time, the replacing misfortunes are prolonged and basis currents (or voltages) include many swells. Implementation of the advanced hysteresis current control band is very much essential for grid related Variable Speed Wind Energy Conversion System (VS-WECS) Antar Beddar *et al.* [3] has proposed fuzzy fractional order PI+I (FFOPI+I) regulator. A Permanent Magnet Synchronous Generator (PMSG) connected through the grid and nonlinear load during a back to back AC-DC-AC PWM converter is prohibited by pertaining the FFOPI+I regulator.

II. PROPOSED MODEL FOR WECS WITH UPQC

The Fig.1 shows the WECS structure which is connected with UPQC and the proposed control methodology. The WECS is implemented to investigate the PMSG operated by a wind turbine, rotor side converter, and a grid side converter [4]. The input from the WECS and non-linear load is improved with the help of the proposed control methodology based on UPQC. The series APF effectively provides the partition between the distribution system and the sub-transmission system with regard to the harmonics also it provides the compensation of voltage flicker/ imbalance and harmonics together with the voltage regulation to occur at the point of common coupling (PCC) [5]. The shunt APF provides compensation, when the load current harmonics and the imbalances in the reactive power as well as the load current. In addition, the series APF facilitates the regulation of voltage from the DC link capacitor.

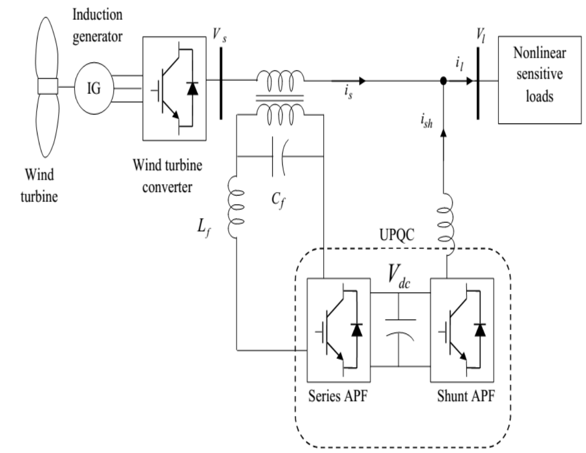

Fig. 1. Structure of the WECS with UPQC and proposed controller

A. *An Overview of WECS*

The wind turbine is successfully employed for the principle of renovating the wind speed into automatic energy. The automatic power is suitably distinct [6] in equation (1),

$$P_m = \frac{1}{2}\rho A C_p(\lambda,\beta)V_\omega^3 \quad (1)$$

Where, P_m symbolizes the automatic productivity power of the wind turbine, ρ , the air compactness, A, the region removed by blades, V_ω, the wind speed in m/s , β , the pitch angle in degree, and $C_p(\lambda,\beta)$, the power coefficient of the wind turbine, The power coefficient is assessed [7] by equation 2 specified as beneath,

$$C_p = 0.73\left(\frac{151}{\lambda_i} - 0.58\beta - 0.002\beta^{2.14} - 13.2\right)e^{-18.4/\lambda_i} \quad (2)$$

$$\lambda_i = \left(\frac{1}{\lambda - 0.002\beta} - \frac{0.003}{\beta^3 + 1}\right)^{-1}$$

At this point, C_p signifies a non-linear task of in cooperation the Tip Speed Ratio (TSR) λ and the pitch angle β.

The obligatory TSR may be predictable by the aid of subsequent equation (3),

$$\lambda = \frac{\omega_r r}{V_\omega} \quad (3)$$

Where, r communicate to the wind turbine blade tip radius and ω_r , the turbine speed. The electrical torque (T_e) and the mechanical torque (T_m) are declared [8] in equations (4) and (5),

$$T_m = \frac{P_m}{\omega_r} \quad (4)$$

$$T_e = \frac{P_e}{\omega_e} = \frac{2}{p}\frac{P_e}{\omega_r} \quad (5)$$

Where, ω_e indicate the electrical angular frequency and p is the quantity of poles.

B. *UPQC power flow analysis*

The series APF and the shunt APF are engaged to modify the load voltage and basis current. The basis voltage, the fatal voltage and the load voltage are distinguished as V_s and V_{ch} in the array. The basis current with the load current are signified as i_s and i_{ch} simultaneously [10]. The injected voltage of the series APF is represented by V_c and the injected current of the shunt APF is represented by i_f. The voltage introduced from the series APF is obtained as the orientation load voltage V_{ch} and the power feature of the load is symbolized as $\cos\phi(n)$.

$$v_c = v_{ch} - v_s = -kV_{ch}\angle 0^0 \quad (6)$$

Then it can be solved using the equation (7),

$$k = \frac{V_s - V_{ch}}{V_{ch}} \quad (7)$$

Let us consider the UPQC as lossless and the power requirement of the load and the active power input of the PCC are equal. Then, the current of the PCC can be described using equation (8),

$$I_s = \frac{I_{ch}}{1+k}\cos\phi_n \quad (8)$$

The apparent power that the series APF and the shunt APF absorb is described in equations (9) and (10) [10].

$$S_c = P_c + jQ_c \quad (9)$$

$$S_f = V_{ch} I_f \quad (10)$$

Here, the active and reactive power is mentioned as equation (11) and (12),

$$P_c = V_c I_s \cos\phi_s \quad (11)$$

$$Q_c = V_c I_s \sin\phi_s \quad (12)$$

Where, P_c and Q_c are the dynamic and the immediate powers that series APF attract; I_f is the dissimilarity among the input basis current and the load current, which includes the load harmonics current simultaneously through the immediate current.

C. *Modelling of the Series APF and Shunt APF controllers*

In the series APF regulator, the Phase Locked Loop (PLL) is successfully used to assess the orientation voltage. The subsequent equations demonstrate the reality that the three segment voltage contribute contain metamorphosed into the d-q axis [9].

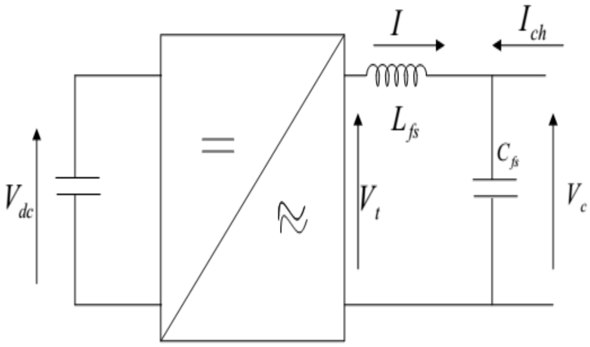

Fig. 2. Structure of series APF control

The three phase voltage supply into the d-q axis is illustrated in equation (13),

$$\begin{bmatrix} V_0 \\ V_d \\ V_q \end{bmatrix} = \frac{2}{3}\begin{bmatrix} 1/2 & 1/2 & 1/2 \\ \sin(\alpha t) & \sin(\alpha t - \frac{2\pi}{3}) & \sin(\alpha t + \frac{2\pi}{3}) \\ \cos(\alpha t) & \cos(\alpha t - \frac{2\pi}{3}) & \cos(\alpha t + \frac{2\pi}{3}) \end{bmatrix}\begin{bmatrix} V_a \\ V_b \\ V_c \end{bmatrix} \quad (13)$$

Where, V_d and V_q stand for the voltages of the axes d and q , correspondingly; V_a, V_b and V_c communicate to the three segment voltages. The orientation voltage is considered by the converse $d-q$ renovation block, which is stated in the subsequent equation (14) as,

$$\begin{bmatrix} V_{Ra} \\ V_{Rb} \\ V_{Rc} \end{bmatrix} = \frac{2}{3}\begin{bmatrix} \sin(\alpha t) & \cos(\alpha t) & 1 \\ \sin(\alpha t - \frac{2\pi}{3}) & \sin(\alpha t + \frac{2\pi}{3}) & 1 \\ \cos(\alpha t - \frac{2\pi}{3}) & \cos(\alpha t + \frac{2\pi}{3}) & 1 \end{bmatrix}\begin{bmatrix} V_d(DC) \\ V_q \\ V_0 \end{bmatrix} \quad (14)$$

Where, V_{Ra}, V_{Rb} and V_{Rc} are the three segment orientation voltages. The hysteresis band of the voltage is prohibited by the control pulses that are derived from the FFA technique. In the shunt APF control representation instant three segment currents and voltages $a-b-c$ are altered into $\alpha-\beta$ as depicted in equation (15) and equation (16),

$$\begin{bmatrix} V_{s0} \\ V_{s\alpha} \\ V_{s\beta} \end{bmatrix} = \sqrt{\frac{2}{3}}\begin{bmatrix} 1/\sqrt{2} & 1/\sqrt{2} & 1/\sqrt{2} \\ 1 & -1/2 & -1/2 \\ 0 & \sqrt{3}/2 & -\sqrt{3}/2 \end{bmatrix}\begin{bmatrix} V_{sa} \\ V_{sb} \\ V_{sc} \end{bmatrix} \quad (15)$$

$$\begin{bmatrix} I_{L0} \\ I_{L\alpha} \\ I_{L\beta} \end{bmatrix} = \sqrt{\frac{2}{3}} \begin{bmatrix} 1/\sqrt{2} & 1/\sqrt{2} & 1/\sqrt{2} \\ 1 & -1/2 & -1/2 \\ 0 & \sqrt{3}/2 & -\sqrt{3}/2 \end{bmatrix} \begin{bmatrix} I_{La} \\ I_{Lb} \\ I_{Lc} \end{bmatrix} \quad (16)$$

Where, V_{sa}, V_{sb} and V_{sc} symbolize the three segment contribute voltages; $V_{s\alpha}$ and $V_{s\beta}$ denote the segment neutral voltages; I_{La}, I_{Lb} and I_{Lc} relay to the three segment load currents; $I_{L\alpha}$ and $I_{L\beta}$ expose the segment work out by the aid of the load currents in concert through the segment neutral voltages.

$$\begin{bmatrix} p \\ q \end{bmatrix} = \begin{bmatrix} V_{s\alpha} & V_{s\beta} \\ -V_{s\beta} & V_{s\alpha} \end{bmatrix} \begin{bmatrix} I_{L\alpha} \\ I_{L\beta} \end{bmatrix} \quad (17)$$

Then, the reference currents can be calculated using the equation (18),

$$\begin{bmatrix} I_{Ra} \\ I_{Rb} \\ I_{Rc} \end{bmatrix} = \sqrt{\frac{2}{3}} \begin{bmatrix} 1 & 0 \\ -1/2 & \sqrt{3}/2 \\ -1/2 & -\sqrt{3}/2 \end{bmatrix} \begin{bmatrix} I_{R\alpha} \\ I_{R\beta} \end{bmatrix} \quad (18)$$

Here I_{Ra}, I_{Rb} and I_{Rc} represents the currents in the orientation of three segment shunt dynamic power filters.

D. Control Pulse Generation using FFA with RNN

Fireflies utilize flash signals to magnetize further fireflies for prospective mates [11]. The entire fireflies are measured unisexual and their magnetism is openly comparative to the concentration of their flash. Consequently, if a firefly element encompasses the alternative of affecting to either of two fireflies, it will be extra concerned to the firefly by superior brightness and shift in that track. If there are no fireflies close by, the firefly will shift in an arbitrary course. The brightness of flash is related through the fitness utility. In firefly algorithm, there are three idealized regulations:

- A firefly will be attracted by other fireflies regardless of their sex.
- Attractiveness is proportional to their brightness and decreases as the distance among them increases.
- The landscape of the objective function determines the brightness of a firefly.

For appropriate intend of FFA, two vital problems are required to be distinct: the dissimilarity of light intensity (I) and the formulation of magnetism (β). Preliminary populace of fireflies in the magnetism of a firefly is given by equation (19) its light intensity or brightness and the brightness are related by the goal task.

$$X_i = [X_1, X_2, X_3, \ldots, X_n] \quad (19)$$

Where, X_i describe the magnetism of the i^{th} firefly. The firefly finest manage pulses are assess by means of equation (20),

$$\varphi = Min\left(S^{ref} - S^{act}\right) \quad (20)$$

Where, S^{ref} and S^{act} symbolize the orientation and definite values of mutually the voltage and current. The light intensity $I(r)$ differ by the detachment r monotonically and exponentially as equation (21),

$$I(r) = I_0 e^{\varphi r} \quad (21)$$

Where, I_0 is the innovative light intensity and φ is the light incorporation coefficient.

$$\beta = \beta_0 e^{-\varphi r^2} \quad (22)$$

Where, β_0 is the magnetism at $r = 0$. The detachment among some two fireflies x_i and x_j is convey as the Euclidean detachment by the support firefly algorithm as equation (23),

$$r_{ij} = \left\| x_i - x_j \right\| = \sqrt{\sum_{k=1}^{n} \left(x_{ik} - x_{jk}\right)^2} \quad (23)$$

Where, n indicate the dimensionality of the difficulty. The progress of the i^{th} firefly is concerned to an additional extra beautiful firefly j.

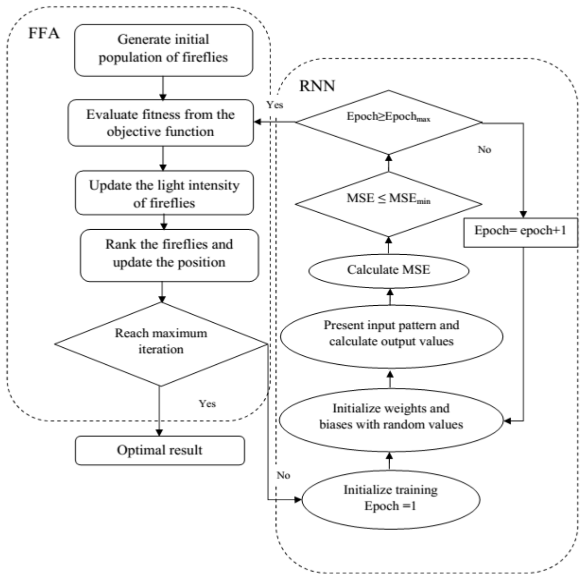

Fig. 3. Structure of series APF control

III. RESULTS AND DISCUSSION

A FFA-RNN supported UPQC associated WECS is proposed concerning the PQ problem introduced by non linear load. The process is assessed for the period of the voltage sag and investigated their consequences in two segments, such as Voltage Sag in unbalanced state and in balanced state.

A. Voltage Sag in the balanced condition

The voltage sag is analyzed under balanced condition and the supply voltage and current is generated as shown in Fig.5. As observed, the amplitude of supply voltage is decreased about 25% from its nominal voltage and the voltage sag is not reduced appropriately. By using UPQC controller based algorithm, the voltage sag is compensated and their performance is described. The injected load current and the load voltages are illustrated in the Fig. 6.

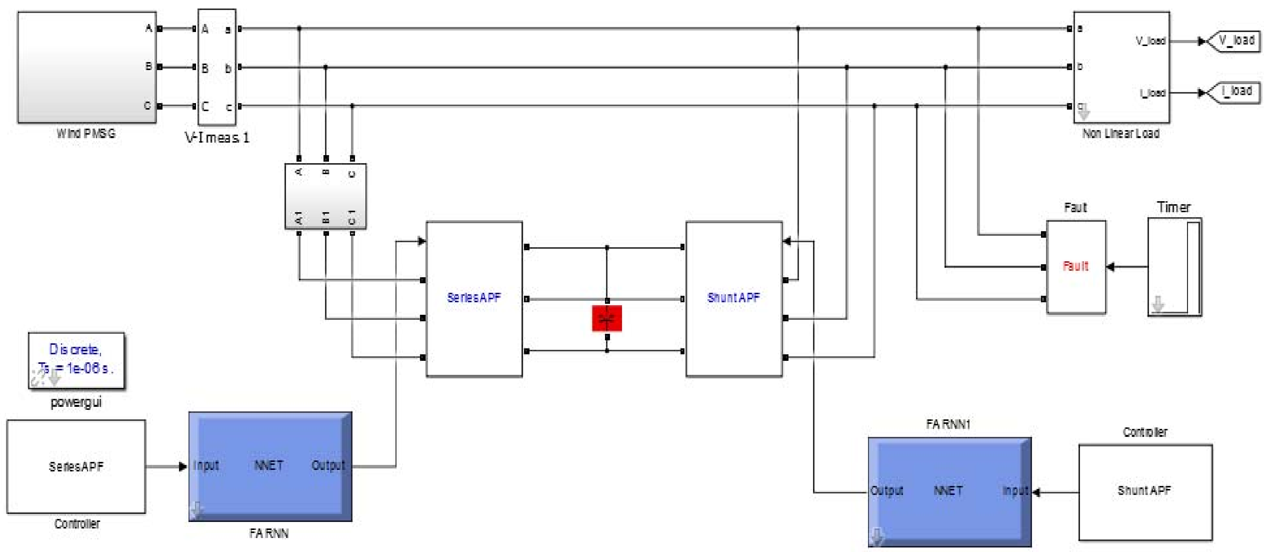

(a)

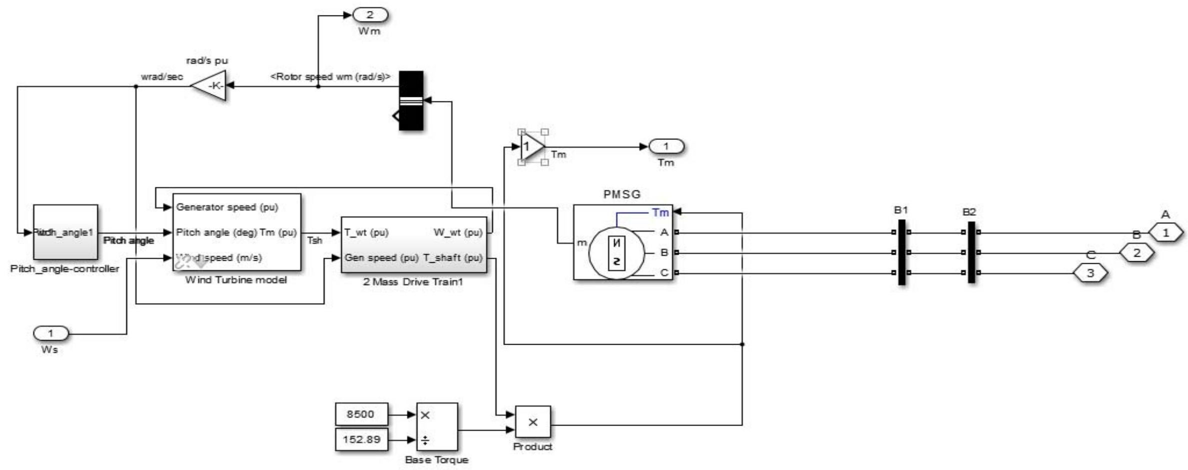

(b)

Fig. 4. Simulink model of (a) proposed controller and (b) PMSG controller

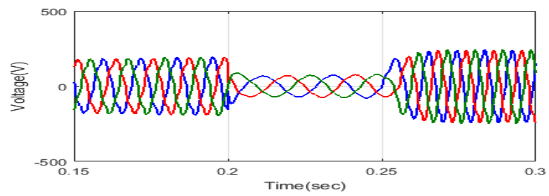

(a)

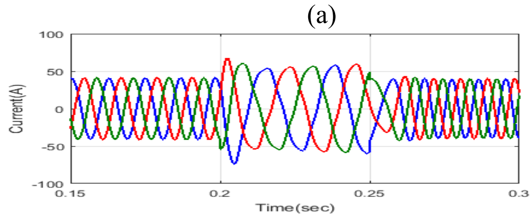

(b)

Fig. 5. Performance analysis of (a) source voltage and (b) source current controll

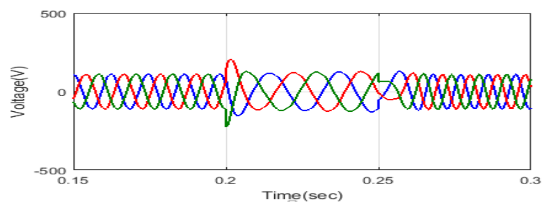

(a)

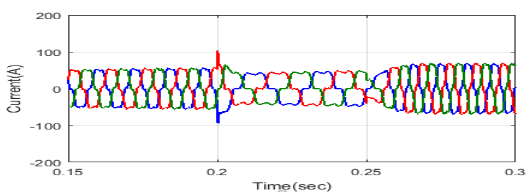

(b)

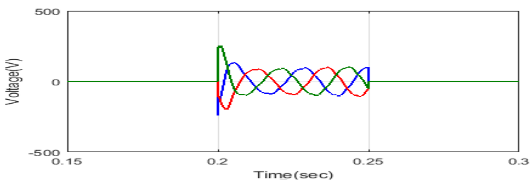

(c)

Fig. 6. Performance analysis of (a) Load voltage (b) Load Current and (c) injected voltage using Proposed Method

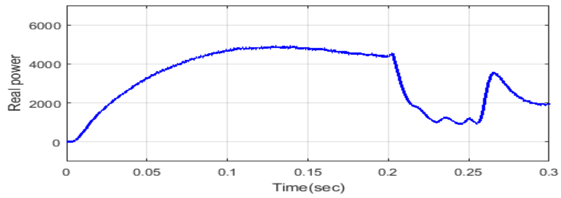

(a)

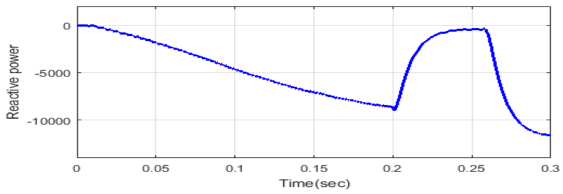

(b)

Fig. 7. Performance analysis of (a) active power and (b) reactive power using proposed method

As it observed from the results, the load voltage is kept at the nominal value with the help of a control algorithm based UPQC. When compared with other techniques, the voltage sag is compensated more efficiently with respect to time by given proposed method. The active and reactive power of the proposed method with balanced condition is shown in Fig. 7.

B. Voltage Sag in unbalanced Condition

This section analyses the voltage sag in unbalanced condition by utilizing the proposed method with various parameters. In order to verify the operating performance of the proposed algorithm based UPQC with power generation in a distribution system is analyzed. The Fig.8 shows the waveform of supply voltage and supply current in unbalanced condition. Moreover, the voltages of the existing methods are analyzed and illustrated in the Fig.9, which are compared with the proposed methods.

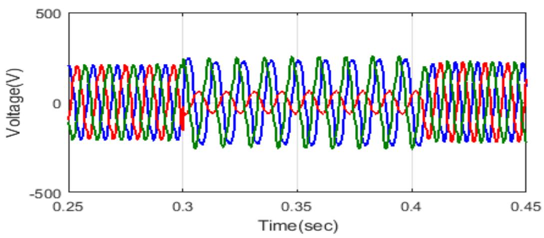

(a)

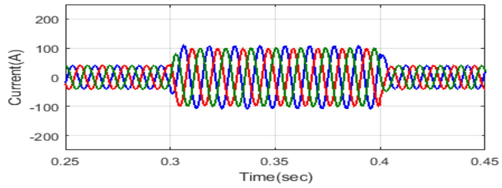

(b)

Fig. 8. Analysis of (a) supply voltage and (b) current

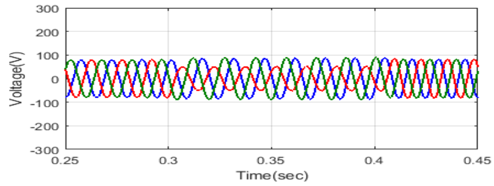

(a)

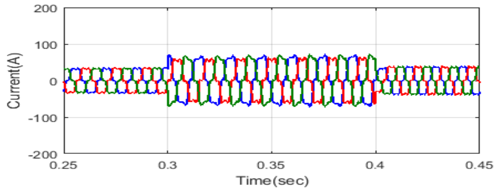

(b)

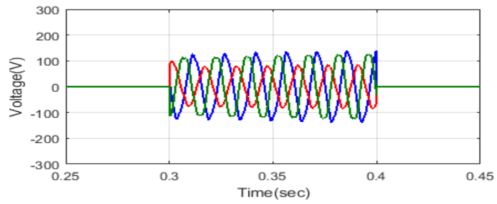

(c)

Fig. 9. Analysis of (a) load voltage (b) load current (c) injected voltage using proposed method with unbalanced condition

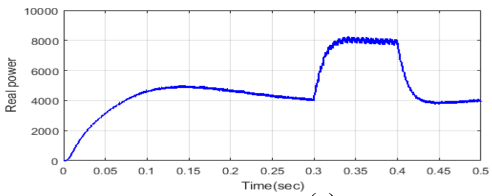

(a)

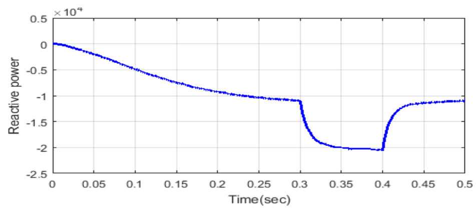

(b)

Fig. 10. Analysis of (a) active power and (b) reactive power using proposed method

Based on the performance of the proposed method with unbalanced condition is slightly better than the other methods. Fig.10. describes the active and reactive power of the proposed system with unbalanced condition.

C. *Comparison analysis of the proposed method*

The efficiency of the projected methodology is compared with GA supported UPQC regulator and ANFIS supported UPQC regulator.

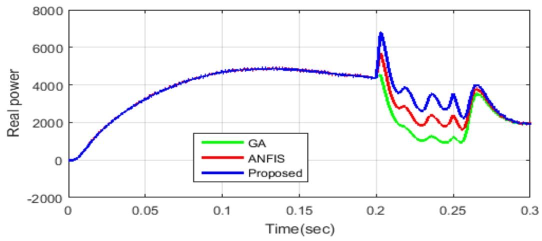

(a)

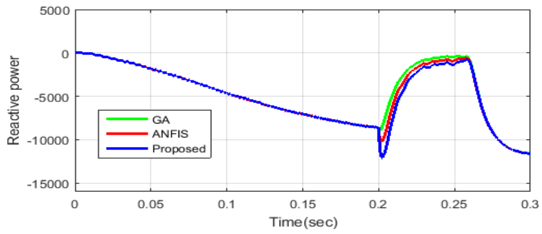

(b)

Fig. 11. comparison analysis of proposed method with (a) active power and (b) reactive power in balanced condition

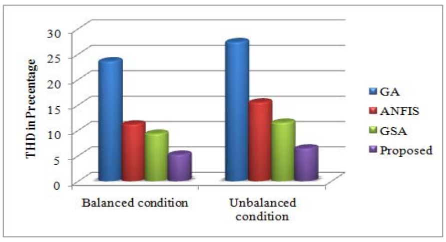

Fig. 12. Performance analysis of THD

In FFT study, THD values of projected regulator compared over GSA supported UPQC, ANFIS supported UPQC and GA supported UPQC is shown in Fig. 12.

IV. CONCLUSION

The FFA-RNN based UPQC is proposed to compensate the voltage sag problem and the simulation results are compared with the existing methodologies. It generates the optimal control pulses to the series and shunt APF based on the source side and load side parameters. These source and load side parameters are considered as the input of the proposed method. The minimum error values are calculated and evaluated system performances. In the proposed controller, the load currents are analyzed with various time instants and their performances are illustrated. It is clearly indicated from THD comparative analysis that the proposed methodology gives the efficient solution to the power quality problems in contrast with the existing algorithms.

REFERENCES

[1] G. Rasit Ata, "Artificial neural networks applications in wind energy systems: a review", An International Journal of Renewable and Sustainable Energy Reviews, Vol.49, pp.534–562, 2015.

[2] R. J. Wenxian Yang and Sunny W.Tian, "Research on a power quality monitoring technique for individual wind turbines", An International Journal of Renewable Energy, Vol.75, pp.187-198, 2015.

[3] Antar Beddar, Hacene Bouzekri, Badreddine Babes and Hamza Afghoul, "Experimental enhancement of fuzzy fractional order PI+I controller of grid connected variable speed wind energy conversion system", An International Journal of Energy Conversion and Management, Vol.123, pp.569–580, 2016.

[4] A.Jayaprakash and D.Jananisri, "Grid connected renewable energy system using unified power quality conditioner for improving power quality", An International Journal of Innovative Research in Computer and Communication Engineering, Vol.2, No.1, 2014.

[5] G.Laxminarayana and G.Umesh Kumar, "Power Quality Improvement Using UPQC for Wind Farm Generation System", An International Journal of Advanced Research in Electrical, Electronics and Instrumentation Engineering, Vol.1, No.6, 2012.

[6] EaswaraMoorthy Nanda Kumar, R. Dhanasekaran and Sundararaj Nanda Kumar, "Simulation of Optimal Power Flow incorporating with Fuzzy Logic Control and various FACTS Devices", An International Journal of Scientific and Research Publications, Vol.2, No.5,pp.1-5, 2012.

[7] Lata Gidwani, Harpal Tiwari and R.C.Bansal, "Improving power quality of wind energy conversion system with unconventional power electronic interface", An International Journal of Electrical Power and Energy Systems, Vol.44, pp.445-453, 2013.

[8] Whei-Min Lin and Chih-Ming Hong, "Intelligent approach to maximum power point tracking control strategy for variable-speed wind turbine generation system", An International Journal of Energy, Vol.35, pp.2440-2447, 2010.

[9] M.Kesraoui, N.Korichi and A.Belkadi, "Maximum power point tracker of wind energy conversion system", An International Journal of Renewable Energy, Vol.36, pp.2655-2662, 2011

[10] P.Balachennaiah, M.Suryakalavathi and P.Nagendra, "Firefly algorithm based solution to minimize the real power loss in a power system", Ain Shams Engineering Journal, 2015.

[11] Iztok Fister, Iztok Fister, Xin-She Yang and Janez Brest, "A comprehensive review of firefly algorithms", An International Journal of Swarm and Evolutionary Computation, Vol.13, pp.34–46, 2013.

[12] Y. Yorozu, M. Hirano, K. Oka, and Y. Tagawa, "Electron spectroscopy studies on magneto-optical media and plastic substrate interface," IEEE Transl. J. Magn. Japan, vol. 2, pp. 740-741, August 1987 [Digests 9th Annual Conf. Magnetics Japan, p. 301, 1982].

[13] M. Young, The Technical Writer's Handbook. Mill Valley, CA: University Science, 1989.

[14] Vaisakh.V and Sunilkumar.A.V, "Power-Quality Improvement Features In Grid Interconnection of Wind Energy Source at the Distribution Level", An International Journal of Innovative Research in Advanced Engineering, Vol.1, No.5, 2014.

[15] G.Laxminarayana and G.Umesh Kumar, "Power Quality Improvement Using UPQC for Wind Farm Generation System", An International Journal of Advanced Research in Electrical, Electronics and Instrumentation Engineering, Vol.1, No.6, 2012.

[16] Chiung Hsing Chen, Chih-Ming Hong and Fu-Sheng Cheng, "Intelligent speed sensor less maximum power point tracking control for wind generation system", An International Journal of Electrical Power and Energy Systems, Vol.42, pp.399–407, 2012.

[17] M.Kesraoui, N.Korichi and A.Belkadi, "Maximum power point tracker of wind energy conversion system", An International Journal of Renewable Energy, Vol.36, pp.2655-2662, 2011.